



Li, X. , Fenu, N. , Cochran, S. and Lucas, M. (2021) Comparison of Performance of Ultrasonic Surgical Cutting Devices Incorporating PZT Piezoceramic and Mn:PIN-PMN-PT Piezocrystal. In: IEEE International Ultrasonic Symposium (IUS 2021), Xi'an, China, 11-16 September 2021, ISBN 9780738112091

(doi: [10.1109/IUS52206.2021.9593623](https://doi.org/10.1109/IUS52206.2021.9593623))

This is the Author Accepted Manuscript.

© 2021 IEEE. Personal use of this material is permitted. Permission from IEEE must be obtained for all other uses, in any current or future media, including reprinting/republishing this material for advertising or promotional purposes, creating new collective works, for resale or redistribution to servers or lists, or reuse of any copyrighted component of this work in other works.

There may be differences between this version and the published version. You are advised to consult the publisher's version if you wish to cite from it.

<http://eprints.gla.ac.uk/257494/>

Deposited on: 21 October 2022

Comparison of performance of ultrasonic surgical cutting devices incorporating PZT piezoceramic and Mn:PIN-PMN-PT piezocrystal

Xuan Li
Centre for Medical &
Industrial Ultrasonics,
James Watt School of
Engineering
University of Glasgow
Glasgow, UK
Xuan.Li@glasgow.ac.uk

Nicola Giuseppe Fenu
Centre for Medical &
Industrial Ultrasonics,
James Watt School of
Engineering
University of Glasgow
Glasgow, UK
Nicola.Fenu@glasgow.ac.uk

Sandy Cochran
Centre for Medical &
Industrial Ultrasonics,
James Watt School of
Engineering
University of Glasgow
Glasgow, UK
Sandy.Cochran@glasgow.ac.uk

Margaret Lucas
Centre for Medical &
Industrial Ultrasonics,
James Watt School of
Engineering
University of Glasgow
Glasgow, UK
Margaret.Lucas@glasgow.ac.uk

Abstract—Bolted Langevin-style Transducers (BLT) are widely adopted in ultrasonic surgical devices. A BLT is normally comprised of a stack of piezoelectric $\text{Pb}(\text{Zr}_x\text{Ti}_{1-x})\text{O}_3$ (PZT) rings. Recently, piezoelectric single crystal material Mn-doped $\text{Pb}(\text{In}_{1/2}\text{Nb}_{1/2})\text{O}_3 - \text{Pb}(\text{Mg}_{1/3}\text{Nb}_{2/3})\text{O}_3 - \text{PbTiO}_3$ (Mn:PIN-PMN-PT) has emerged as a potential alternative. Differently from PZT, where a trade-off in material properties is necessary, Mn:PIN-PMN-PT crystal simultaneously exhibits high piezoelectric coefficient, d_{ij} , electromechanical coupling coefficient, k_{ij} , and mechanical quality factor, Q_m . As a result of the higher efficiency, lower electromechanical losses and higher energy density of the piezocrystal material, there is potential for designing smaller ultrasonic devices incorporating Mn:PIN-PMN-PT in BLTs.

A stepped shape horn with a thin and rounded blade, forming a surgical tip, was tuned to its 1st longitudinal mode (L1) at around 20 kHz. Equivalent tips were then attached to the two BLTs, one incorporating the piezoceramic and one employing the piezocrystal material. The full devices were therefore tuned to L2 at 20kHz. The two devices were also excited in the L6 mode at around 60 kHz to investigate the frequency effect on the achievable displacement amplitude at the blade tip. Experimental results show that the Mn:PIN-PMN-PT driven surgical device achieved higher displacement amplitude for the same applied voltage, as a result of the higher power density of the piezocrystal material.

Keywords—Ultrasonic surgical devices, BLT transducer, Piezoceramic, Mn:PIN-PMN-PT crystal

I. INTRODUCTION

The bolted Langevin-style Transducer (BLT) is a common design of power ultrasonic transducers and widely used in ultrasonic surgical devices. A BLT comprises a stack of piezoelectric rings sandwiched between two end masses [1], which are pre-stressed by means of a bolt. The BLT is usually tuned to its 1st longitudinal mode (L1) and operates at a resonance frequency in the range of 20 -100 kHz, delivering an intensity of 10 – 1000 W/cm² [2]. The piezoelectric rings stack are located close to the displacement node to maximise the electromechanical coupling coefficient k_{eff} [3]. A half wavelength horn with a tapered geometry is attached to amplify the vibrational displacement. For an ultrasonic surgical device, the horn incorporates a cutting insert. For a

full wavelength configuration of transducer and horn/cutting tip, the device will be tuned to the L2 mode.

There have been many innovations and performance advancements of ultrasonic surgical devices since their emergence. These include optimisation of the dynamic performance by consideration of the number of piezoceramic rings in the transducer [4], design of different geometries of surgical tips to suit specific procedures [5], [6], and the implementation of different vibration modes of surgical tips [7], [8]. However, the use of hard piezoceramic material in the transducer has remained unchanged.

Piezoelectric single crystal material, such as Mn-doped $\text{Pb}(\text{In}_{1/2}\text{Nb}_{1/2})\text{O}_3 - \text{Pb}(\text{Mg}_{1/3}\text{Nb}_{2/3}) - \text{PbTiO}_3$ (Mn:PIN-PMN-PT), has recently emerged as a potential alternative to the existing hard piezoceramic material for use in power ultrasonic applications, due to its extraordinary material properties. Compared to hard piezoceramic material, relaxor-based piezoelectric single crystal shows simultaneously high piezoelectric coefficient d_{ij} , electromechanical coupling coefficient k_{ij} , mechanical quality factor Q_m [9], [10], and higher energy density. This creates an opportunity to explore the potential of using piezocrystal material in the transducers, especially for enabling design of smaller ultrasonic surgical devices.

II. ULTRASONICS SURGICAL DEVICES

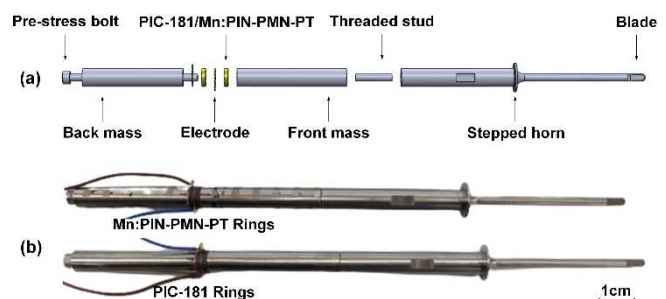


Fig. 1. (a) Exploded view of the ultrasonic surgical device, (b) 20 kHz full-wavelength ultrasonic surgical devices embedding PZT and Mn:PIN-PMN-PT rings

Fig. 1 (a) presents the structure of a half wavelength BLT, incorporating either a pair of hard piezoceramic rings PIC-181 (PI Ceramic, Lederhose, Germany) or a pair of Mn:PIN-PMN-PT piezocrystal rings (TRS Technologies, State College, PA,

USA). Both sets of rings have dimensions of OD 10 mm, ID 5 mm, thickness 2 mm. A stepped horn with a thin (0.5 mm thickness) and rounded shape blade ($\varnothing 4$ mm) is attached to the transducer via a threaded stud to form a slender shape ultrasonic surgical tool. A 1 mm thickness flange is located at the step in the horn at a displacement node, to allow for attachment to a housing for tissue cutting experiments.

The manufactured stepped horn is shown in Fig. 1 (b). Identical horns are connected to the two BLTs. Due to the lower compliance of the Mn:PIN-PMN-PT piezocrystal material, the length of this device is approximately 10 mm shorter than the PZT actuated surgical device so that they are both tuned at the same resonance frequency. The two devices vibrate in their L2 modes at around 20 kHz. In this study they are also excited in their L6 modes at around 60 kHz, to compare the resonance frequency effect on the achievable displacement amplitude of the two cutting devices. The acoustic power consumption is also considered in order to understand the effects of the different energy density of the two piezoelectric materials.

III. RESULTS AND DISCUSSION

A. Electrical impedance

The electrical impedance of both surgical tools was measured using an impedance analyser (Agilent 4294A, Agilent Technologies, CA, USA). A swept signal of 1 V peak-to-peak over a bandwidth of interest was applied and the impedance spectrum was measured. From the impedance spectrum data, the effective coupling coefficient k_{eff} was calculated using equation (1) [11], and the mechanical Q factor was also calculated.

$$k_{\text{eff}}^2 = \frac{f_a^2 - f_r^2}{f_a^2} \quad (1)$$

f_r is the resonance frequency and f_a is the anti-resonance frequency.

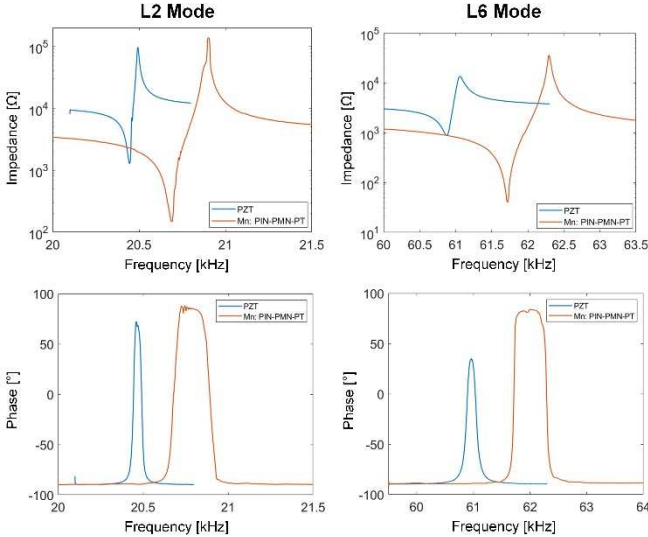


Fig. 2. Impedance magnitude and phase characteristics of the two ultrasonic surgical devices in the L2 and L6 modes

Impedance magnitude and phase responses of the two ultrasonic surgical devices driven in their L2 and L6 modes are presented in Fig. 2, and the extracted parameters are summarised in TABLE I.

TABLE I. PROPERTIES OF TWO SURGICAL DEVICES

Device	PZT	
Mode	L2	L6
f_r [Hz]	20446	60876
f_a [Hz]	20493	61058
Z [Ω at f_r]	1275	881
θ [$^\circ$ at f_r]	12	-25
k_{eff}	0.068	0.077
Q	1216	586
Device	Mn:PIN-PMN-PT	
Mode	L2	L6
f_r [Hz]	20691	61716
f_a [Hz]	20900	62290
Z [Ω at f_r]	147	40
θ [$^\circ$ at f_r]	27	3
k_{eff}	0.141	0.135
Q	941	1763

Impedance magnitude and phase characteristics of the Mn:PIN-PMN-PT device exhibit a wider bandwidth for both modes, resulting in a larger coupling coefficient k_{eff} . As seen in TABLE I, the values are twice as high as for the PZT device. The Q factors of both devices for the L2 mode show a similar value, of around 1000. However, the PZT device exhibits higher damping in the L6 mode, three time higher than the Mn:PIN-PMN-PT device. This demonstrates the potential of the Mn:PIN-PMN-PT material to achieve a device with simultaneously high k_{eff} and high Q. The impedance magnitude of the PZT device is around a kilo-ohm in both modes, ten times higher than for the Mn:PIN-PMN-PT device.

B. Mode shapes

The vibration mode shapes of the surgical devices are measured using experimental modal analysis (EMA). EMA was performed by measuring the frequency response functions (FRFs) from a grid of vibration response measurement points along an axial line on the surface of the devices. From the EMA the modal parameters, resonance frequency, damping and mode shape, can be extracted. A white noise signal of 10 V was generated by a signal generator (Quattro, Data Physics, Santa Clara, CA, USA) and then amplified by a power amplifier (QSC RMX 4050HD, Costa Mesa, CA, USA), before being supplied to the piezoelectric materials. A 3D laser Doppler vibrometer (CLV3000, Polytec GmbH, Waldbronn, Germany) was used to measure three orthogonal components of the vibration velocity of the grid points. Data acquisition and processing software (SignalCalc, Data Physics, Santa Clara, CA, USA) was used to calculate the FRFs and then to apply curve-fitting functions to calculate the magnitude and phase data. Lastly, the FRFs were exported to modal analysis software (MEscopeVES, Vibrant Technology Inc., Centennial, CO, USA) to extract the modal parameters.

Fig. 3 shows the extracted vibration mode shapes of the two surgical devices in the L2 and L6 modes from FEA simulation and EMA experiments.

The predicted results and EMA measurements show a close agreement with respect to the resonance frequencies, position of the displacement nodes and the amplitude gain (defined as a ratio of the displacement amplitude at the tip of the blade and the end of the back mass).

Damping was also calculated from EMA measurements, showing a Q factor of 1714 and 1205 for the L2 mode, and 1478 and 682 for the L6 mode for the PZT device and

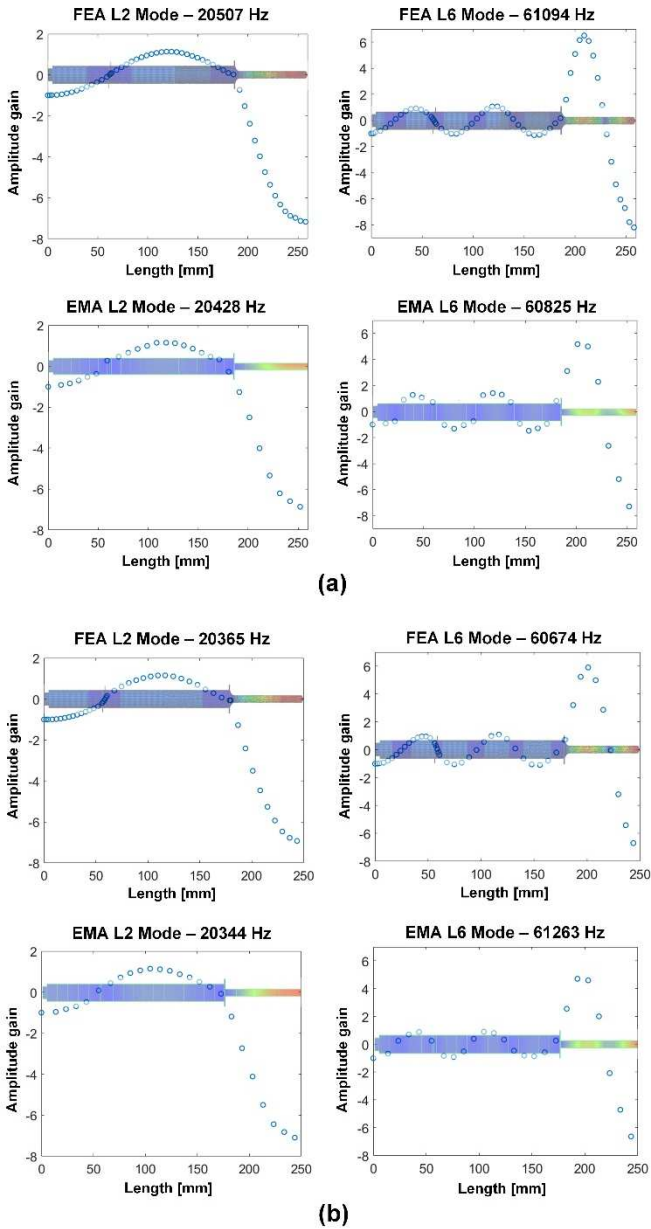


Fig. 3. Extracted vibration mode shapes from FEA and EMA: (a) PZT device, (b) Mn:PIN-PMN-PT device

Mn:PIN-PMN-PT device, respectively. The Q values from EMA are 20-30% higher than those estimated from impedance measurements for the L2 mode. However, in the L6 mode one Q value is much higher and the other much lower. This supports other studies that show that estimation of Q is very affected by the type of measurement and excitation level [4].

C. Vibration response

To compare the dynamic behaviours of the two devices, they were excited via a frequency sweep through a range from below to above the resonance frequency, using a burst sine signal generated from a signal generator (Agilent 33210A, Agilent Technologies, USA) and amplified by a power amplifier (HFVA-62, Foneng Technology Industry Co., China). The longitudinal vibration response was measured using a 1D laser Doppler vibrometer (OFV 303, Polytec GmbH, Germany) at the tip of the blade. To minimise heating, each burst sine signal had a fixed 6000 oscillation cycles, and 2 s between sequential bursts. Vibration response data were

captured with a 5 Hz resolution, and the applied voltage was stepped from 1 V, then in increments of 10 Vrms up to a voltage that developed no further amplitude.

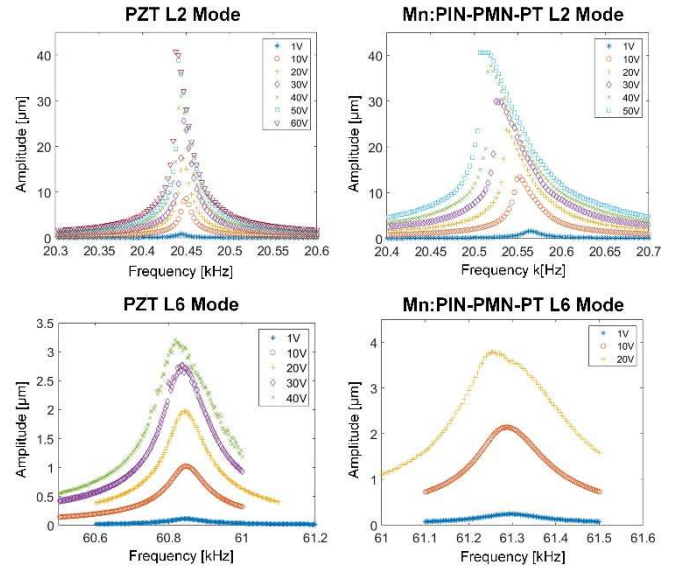


Fig. 4. Vibration characteristics of the ultrasonic surgical devices driven in the L2 and L6 modes

The displacement amplitude-frequency responses of the devices excited in L2 and L6 modes are presented in Fig. 4.

The maximal displacement amplitude is slightly over 40 μm in the L2 mode and around 3.5 μm in the L6 mode for both devices, which however, are achieved at different applied voltage levels. A very weak softening nonlinear responses is observed in all the responses [12], with the Mn:PIN-PMN-PT device showing a slightly larger reduction in resonance frequencies for increasing excitation. This is partly due to the practical difficulty in aligning the orientation of Mn:PIN-PMN-PT rings in the device correctly, due to the complex thickness vibration mode shape compared to the more uniform thickness mode shape of the PZT rings [13]. This introduces a small piezoelectric loss at the higher excitations.

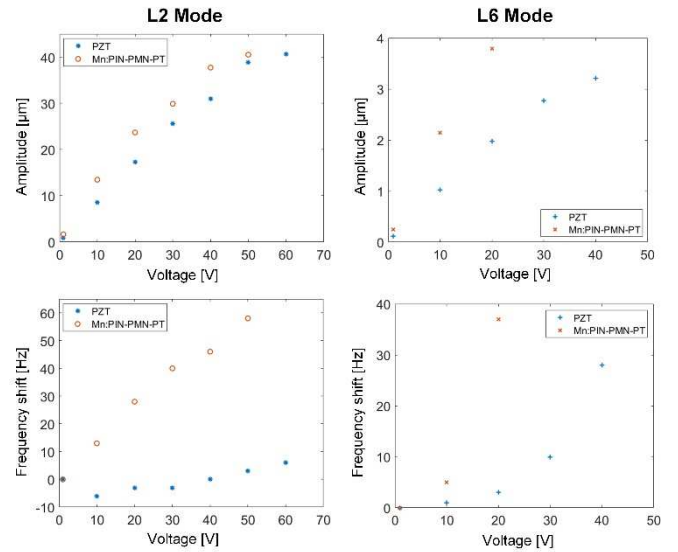


Fig. 5. Vibration characteristics of the ultrasonic surgical devices in the L2 and L6 modes

To further interrogate the data from Fig. 4, the maximal recorded amplitude at the tip of the blade and the resonance

frequency shifts at each excitation level are calculated and plotted in Fig. 5.

For the same applied voltage, the Mn:PIN-PMN-PT device achieved a higher displacement amplitude at the blade tip than the PZT device. However, saturation was reached at 60 V for the PZT device and 50 V for Mn:PIN-PMN-PT device in the L2 mode, and 40 V and 20 V in the L6 mode, which was due to the intrinsic difference in the impedance magnitude and piezoelectric properties of the two materials. Considering the gain values (7 to 8 in Fig. 3), a larger displacement amplitude was expected at the blade tip in the L2 mode. However, the displacement amplitude was limited by the small number of piezoelectric rings [4]. This also meant that in the L6 mode the displacement amplitude was only 3 to 4 μm .

In terms of the resonance frequencies, the PZT device presents almost no change in the L2 mode as opposed to a 60 Hz frequency shift for the Mn:PIN-PMN-PT device. In the L6 mode, Mn:PIN-PMN-PT device has developed a 40 Hz frequency shift at 20 V, where the value is slightly under 30 Hz at a 40 V for the PZT device.

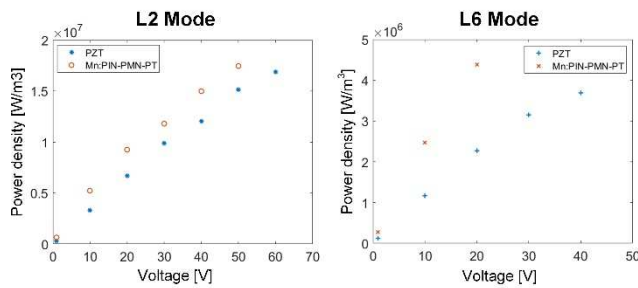


Fig. 6. Power density at different excitation levels for two devices in the L2 and L6 modes

To understand the active power transfer per unit volume of PZT and Mn:PIN-PMN-PT material, power density at different excitation levels for both surgical devices in the L2 and L6 modes was calculated using equation (2),:

$$P_d = \frac{UI \cos \theta}{V} \quad (2)$$

P_d is the power density, U is the amplitude of voltage, I is the amplitude of current, θ is the phase angle between voltage and current, and V is the volume of one pair of piezoelectric rings ($2.356 \times 10^{-7} \text{ m}^3$). Results are shown in Fig. 6.

For both devices, the power density in the L2 mode is higher than L6 mode, and the Mn:PIN-PMN-PT device has a higher power density than the PZT device. This contributes to the higher displacement amplitude achieved at the same excitation voltage level for the Mn:PIN-PMN-PT device in Fig. 5.

IV. CONCLUSION AND FUTURE WORK

Two identical stepped horns with a thin and rounded blade, tuned to the 1st longitudinal mode (L1) at around 20 kHz, were manufactured and then attached to two BLTs, one incorporating a hard PZT and the other Mn:PIN-PMN-PT piezoelectric materials. The two BLTs are tuned to the same resonance frequency as the horn to constitute two slender ultrasonic surgical devices tuned to their L2 mode.

Preliminary results show that the Mn:PIN-PMN-PT device presents a simultaneously high Q and high k_{eff}

compared to the hard PZT device in the L2 mode, resulting in a higher displacement amplitude at the tip of the blade at the same input voltage. However, the Mn:PIN-PMN-PT device presents a slightly larger resonance frequency decrease for increasing excitation, due to the misalignment of the orientation of the Mn:PIN-PMN-PT rings in the thickness mode, which presents a more complex shape than the more uniform thickness mode of the PZT rings. Displacement amplitude in the L6 mode for both devices is very low, which is due to the small number of piezoelectric rings in the structure. The power density demonstrates that the Mn:PIN-PMN-PT device has consumed higher power at the same voltage than the PZT device, due to the lower impedance and higher power density of the Mn:PIN-PMN-PT material. Tissue cutting experiments will be conducted to evaluate the performance of these two ultrasonic surgical devices.

REFERENCES

- [1] D. A. DeAngelis, G. W. Schulze, and K. S. Wong, "Optimizing Piezoelectric Stack Preload Bolts in Ultrasonic Transducers," *Physics Procedia*, vol. 63, pp. 11–20, 2015.
- [2] A. Mathieson, A. Cardoni, N. Cerisola, and M. Lucas, "Understanding nonlinear vibration behaviours in high-power ultrasonic surgical devices," *Proceeding of the Royal Society A: Mathematical, Physical and Engineering Sciences*, vol. 471, no. 2176, 2015.
- [3] V. K. Astashev, K. A. Pichugin, X. Li, A. Meadows, and V. I. Babitsky, "Resonant tuning of Langevin transducers for ultrasonically assisted machining applications," *IEEE Transactions on Ultrasonics, Ferroelectrics, and Frequency Control*, vol. 67, no. 9, pp. 1888–1896, 2020.
- [4] X. Li, T. Stritch, K. Manley, and M. Lucas, "Limits and opportunities for miniaturising ultrasonic surgical devices based on a Langevin transducer," *IEEE Transactions on Ultrasonics, Ferroelectrics, and Frequency Control*, vol. 68, no. 7, pp. 2543–2553, 2021.
- [5] R. Cox, "Getting the Most Out of Ultrasonic Scaling: A Guide to Maximizing Efficacy," *Academy of General Dentistry*, pp. 1–6, 2015.
- [6] G. Plotino, C. H. Pameijer, N. Maria Grande, and F. Somma, "Ultrasonics in Endodontics: A Review of the Literature," *Journal of Endodontics*, vol. 33, no. 2, pp. 81–95, 2007.
- [7] J. Yang, Q. Zhang, and T. Xu, "A novel piezoelectric ceramic actuator with scissoring composite vibration for medical applications," *Applied Sciences*, vol. 9, no. 21, 2019.
- [8] S. C. Lea, B. Felver, G. Landini, and A. D. Walmsley, "Three-dimensional analyses of ultrasonic scaler oscillations," *Journal of Clinical Periodontology*, vol. 36, no. 1, pp. 44–50, 2009.
- [9] S. Zhang and T. R. Shrout, "Relaxor-PT single crystals: Observations and developments," *IEEE Transactions on Ultrasonics, Ferroelectrics, and Frequency Control*, vol. 57, no. 10, pp. 2138–2146, 2010.
- [10] S. Zhang, F. Li, X. Jiang, J. Kim, J. Luo, and X. Geng, "Advantages and Challenges of Relaxor-PbTiO₃ Ferroelectric Crystals for Electroacoustic Transducers- A Review," *Progress in Materials Science*, vol. 68, pp. 1–66, 2015.
- [11] A. Caronti, R. Carotenuto, and M. Pappalardo, "Electromechanical coupling factor of capacitive micromachined ultrasonic transducers," *The Journal of the Acoustical Society of America*, vol. 113, no. 1, pp. 279–288, 2003.
- [12] A. Mathieson, A. Cardoni, N. Cerisola, and M. Lucas, "The influence of piezoceramic stack location on nonlinear behavior of langevin transducers," *IEEE Transactions on Ultrasonics, Ferroelectrics, and Frequency Control*, vol. 60, no. 6, pp. 1126–1133, 2013.
- [13] N. G. Fenu, X. Li, M. Lucas, and S. Cochran, "Evaluation of PIC 181 and Mn:PIN-PMN-PT thickness extensional rings for use in power ultrasonic devices for minimally invasive surgery," *IEEE International Ultrasonics Symposium (IUS)*, pp. 1–4, 2020.